LOAN DOCUMENT

AD-A239 097

DTIC ACCESSION NUMBER

PHOTOGRAPH THIS SHEET

LEVEL

INVENTORY 1

Protection of a QPSK Communication ... etc

DOCUMENT IDENTIFICATION

Jan 1986

DISTRIBUTION STATEMENT

ACCESSION FOR

NTIS GRA&I ☑

DTIC TRAC ☐

UNANNOUNCED ☐

JUSTIFICATION

BY Per A034095

DISTRIBUTION/

AVAILABILITY CODES

DISTRIBUTION	AVAILABILITY AND/OR SPECIAL
A-1	

DISTRIBUTION STAMP

DTIC

DATE ACCESSIONED

DATE RETURNED

91 Z 30 025

91-06532

DATE RECEIVED IN DTIC

REGISTERED OR CERTIFIED NUMBER

PHOTOGRAPH THIS SHEET AND RETURN TO DTIC-FDAC

DTIC FORM 70A JUN 80

DOCUMENT PROCESSING SHEET

PREVIOUS EDITIONS MAY BE USED UNTIL STOCK IS EXHAUSTED.

LOAN DOCUMENT

HANDLE WITH CARE

The Ohio State University

PROTECTION OF A QPSK COMMUNICATION SYSTEM WITH AN LMS ADAPTIVE ARRAY

by

Matthew W. Ganz

The Ohio State University

ElectroScience Laboratory

Department of Electrical Engineering
Columbus, Ohio 43212

Quarterly Technical Report 717253-2
Contract N00019-85-C-0119
January 1986

Department of the Navy
Naval Air Systems Command
Washington, DC 20416

NOTICES

When Government drawings, specifications, or other data are used for any purpose other than in connection with a definitely related Government procurement operation, the United States Government thereby incurs no responsibility nor any obligation whatsoever, and the fact that the Government may have formulated, furnished, or in any way supplied the said drawings, specifications, or other data, is not to be regarded by implication or otherwise as in any manner licensing the holder or any other person or corporation, or conveying any rights or permission to manufacture, use, or sell any patented invention that may in any way be related thereto.

50272-101

REPORT DOCUMENTATION PAGE	1. REPORT NO. 717253-2	2.	3. Recipient's Accession No.

4. Title and Subtitle
PROTECTION OF A QPSK COMMUNICATION SYSTEM WITH AN LMS ADAPTIVE ARRAY

5. Report Date
January 1986

6.

7. Author(s)
Matthew W. Ganz

8. Performing Organization Rept. No.
717253-2

9. Performing Organization Name and Address
The ElectroScience Laboratory
The Ohio State University
1320 Kinnear Road
Columbus, Ohio 43212

10. Project/Task/Work Unit No.

11. Contract(C) or Grant(G) No
(C) N00019-85-C-0119
(G)

12. Sponsoring Organization Name and Address
Department of the Navy
Naval Air Systems Command
Washington, DC 20416

13. Type of Report & Period Covered
Quarterly

14.

15. Supplementary Notes

16. Abstract (Limit: 200 words)

The performance of a quadrature phase-shift-keyed (QPSK) communication system which uses an adaptive array is examined. The equations that describe the adaptive array and ideal detector performance are derived for the case where the desired signal is corrupted by CW interference. Performance calculations are described which show that the adaptive array offers a significant degree of protection from this type of interference. The effects on performance of the signal frequencies, power levels, arrival angles and the array bandwidth are examined.

17. Document Analysis a. Descriptors

Quadrature Phase Shift Keying
Communications
Adaptive Arrays
Interference

b. Identifiers/Open-Ended Terms

c. COSATI Field/Group

18. Availability Statement	19. Security Class (This Report)	21. No of Pages
APPROVED FOR PUBLIC RELEASE; DISTRIBUTION IS UNLIMITED.	Unclassified	45
	20. Security Class (This Page) Unclassified	22. Price

(See ANSI-Z39.18) See Instructions on Reverse OPTIONAL FORM 272 (4-77) (Formerly NTIS-35) Department of Commerce

TABLE OF CONTENTS

LIST OF FIGURES

I. INTRODUCTION

This report examines the performance of a quadrature phase-shift keyed (QPSK) communication system that uses an adaptive array for interference protection. We assume a QPSK signal is received with an LMS adaptive array [1]. The QPSK signal demodulation is done at the output of the adaptive array. The demodulator is an optimal detector for a QPSK signal in additive white Gaussian noise (AWGN) [2]. We assume the array is subjected to CW (single frequency) interference in addition to the desired QPSK signal. We calculate the bit error probability (BEP) for this system as a function of the desired signal, interference and array parameters.

A previous report [3] considered the analogous problem for binary phase-shift keyed (BPSK) signals. As was pointed out there, most previous studies of adaptive array performance have used the array output signal-to-interference-plus-noise ratio (SINR) to characterize array performance. The SINR is useful for this purpose because it is easily calculated and because the performance of a communication system usually improves with SINR. However, as we showed in [3], when a signal demodulator is subjected to interference in addition to the desired signal, its performance depends on more than just SINR. Other factors that do not appear in this simple power ratio, such as interference frequency, bandwidth, etc., also affect the performance. For this reason, output SINR alone is not sufficient to characterize communication system performance. One must calculate the detector BEP.

In Section II of this report, we briefly describe the adaptive array notation and define the signals. (The reader is refered to [3] for a more complete description of the array.) Section III discusses the performance of an optimal QPSK detector when subjected to CW interference. Section IV describes the performance of the combined adaptive array and QPSK system. Finally, Section V contains our conclusions.

II. THE LMS ADAPTIVE ARRAY

Figure 1 shows a 3-element adaptive array. The elements are assumed equally spaced a half wavelength apart at the desired signal frequency. The QPSK desired signal arrives from angle θ_d and a CW interference signal arrives from angle θ_i, both measured from broadside as shown in Figure 1. The received signal on each element is passed through a bandpass filter (BPF), which establishes the array bandwidth. We denote the analytic signal behind element J (after the filter) by $\tilde{x}_j(t)$. Each $\tilde{x}_j(t)$ is multiplied by a complex weight w_j and the weighted signals are summed to produce the array output signal $\tilde{s}(t)$. The weights are controlled with an adaptive system, such as a set of LMS feedback loops [1]. This system sets the weights to their optimal values,

$$W = \Phi^{-1}S \tag{2.1}$$

where W is the weight vector,

$$W = [W_1, W_2, W_s]^T , \tag{2.2}$$

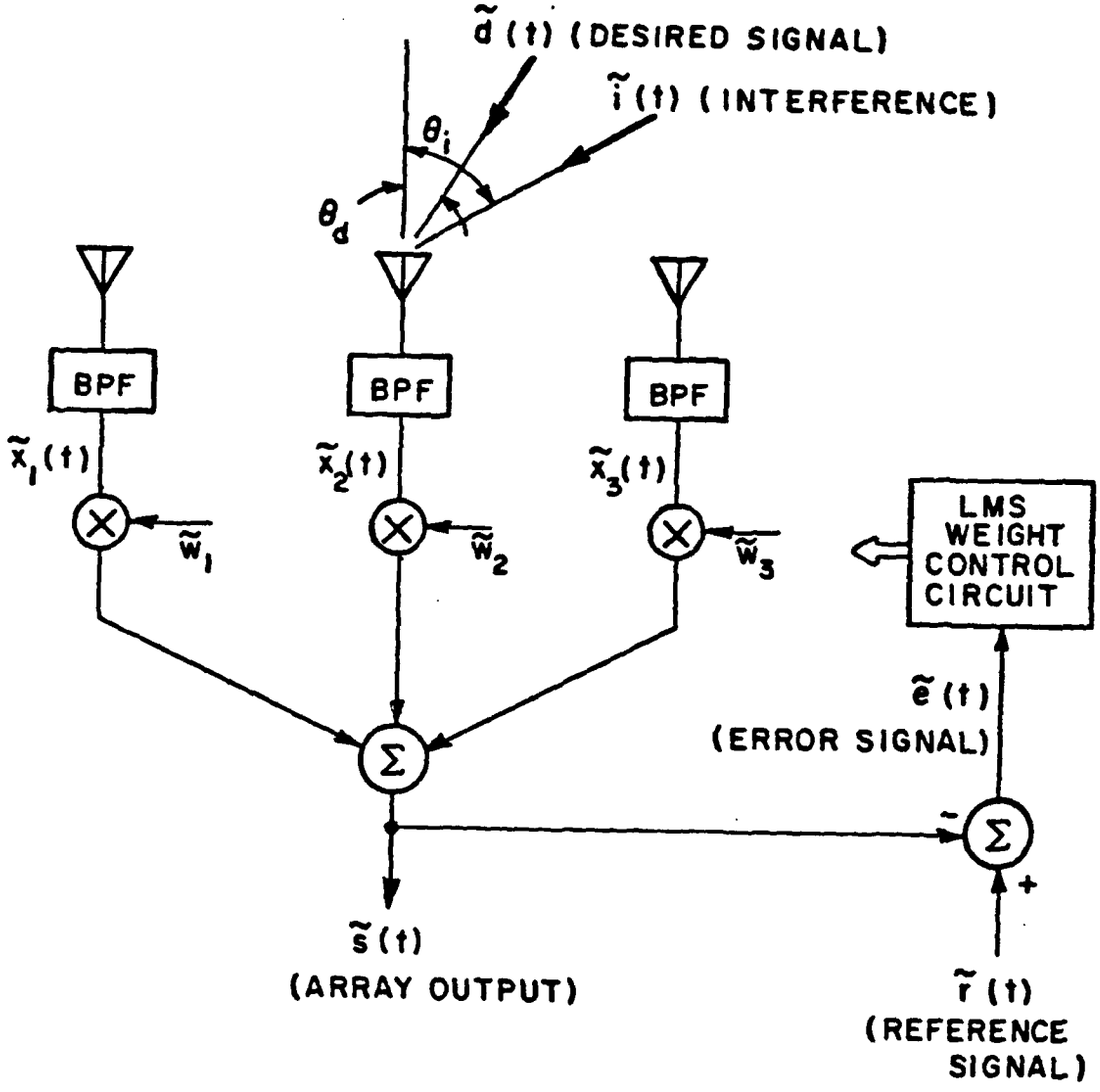

Figure 1. The complex LMS array.

Φ is the covariance matrix,

$$\Phi = E[X^* X^T] \tag{2.3}$$

S is the reference correlation vector,

$$S = E[X^* \tilde{r}(t)], \tag{2.4}$$

and X is the signal vector,

$$X = [\tilde{X}(t), \tilde{X}_2(t), \tilde{X}_3(t)]^T \tag{2.5}$$

In these equations, * denotes complex conjugate, and $\tilde{r}(t)$ is the reference signal (shown in Figure 1), which we assume equal to the desired signal. (In a practical array, the reference signal is derived from the array output. Winters has described one method of doing this with QPSK signals [4].)

To determine the optimal weight vector in (2.1), the first step is to calculate the covariance matrix Φ from the incident signals. We assume that, in addition to the desired and interference signals, each element signal contains an independent thermal noise voltage of power σ^2. The covariance matrix may then be split into three terms (see [3] for more details)

$$\Phi = \Phi_d + \Phi_i + \Phi_n \tag{2.6}$$

where Φ_d, Φ_i and Φ_n are covariance matrices due to desired, interference and noise signals. The desired signal covariance matrix is given by

$$\Phi_d = \begin{bmatrix} R_{\tilde{d}}(0) & R_{\tilde{d}}(-T_d) & R_{\tilde{d}}(-2T_d) \\ R_{\tilde{d}}(T_d) & R_{\tilde{d}}(0) & R_{\tilde{d}}(-T_d) \\ R_{\tilde{d}}(2T_d) & R_{\tilde{d}}(T_d) & R_{\tilde{d}}(0) \end{bmatrix} \tag{2.7}$$

where $R_{\tilde{d}}(T)$ is the autocorrelation function of the desired signal waveform $d(t)$,

$$R_{\tilde{d}}(\tau) = E[\tilde{d}^*(t)\tilde{d}(t+\tau)] \tag{2.8}$$

and T_d is the desired signal interelement propagation time delay,

$$T_d = \frac{L}{c} \sin\theta_d \tag{2.9}$$

with L the distance between elements in Figure 1 and c the velocity of propagation. The interference covariance matrix is

$$\Phi_i = \begin{bmatrix} R_{\tilde{i}}(0) & R_{\tilde{i}}(-T_i) & R_{\tilde{i}}(-2T_i) \\ R_{\tilde{i}}(T_i) & R_{\tilde{i}}(0) & R_{\tilde{i}}(-T_i) \\ R_{\tilde{i}}(2T_i) & R_{\tilde{i}}(T_i) & R_{\tilde{i}}(0) \end{bmatrix} \tag{2.10}$$

where $R_{\tilde{i}}(\tau)$ is the autocorrelation function of the interference waveform $\tilde{i}(t)$,

$$R_{\tilde{i}}(\tau) = E[\tilde{i}^*(t)\tilde{i}(t+\tau)] \tag{2.11}$$

and T_i is the interelement propagation time for the interference signal,

$$T_i = \frac{L}{c} \sin\theta_i \tag{2.12}$$

The noise covariance matrix is simply

$$\Phi_n = \sigma^2 I \tag{2.13}$$

where I is the identity matrix. Finally, since the reference signal is equal to the desired signal $\tilde{d}(t)$, we also find

$$S = \begin{bmatrix} R_{\tilde{d}}(0) \\ R_{\tilde{d}}(T_d) \\ R_{\tilde{d}}(2T_d) \end{bmatrix} \tag{2.14}$$

Once the array weights have been calculated from (2.1), the array output desired signal, interference and noise powers may be found from

$$P_d = \frac{1}{2} \sum_{j=1}^{3} \sum_{k=1}^{3} W_j W_k^* R_{\tilde{d}}[(j-k)T_d], \tag{2.15}$$

$$P_i = \frac{1}{2} \sum_{j=1}^{3} \sum_{k=1}^{3} W_j W_k^* R_{\tilde{i}}[(j-k)T_i], \tag{2.16}$$

and

$$P_n = \frac{\sigma^2}{2} \sum_{j=1}^{3} |W_j|^2 \tag{2.17}$$

The SINR is then given by

$$SINR = \frac{P_d}{P_j + P_n} \tag{2.18}$$

Figure 2 shows a typical QPSK waveform. Each of the four possible QPSK symbols represents two bits of information. Thus, for QPSK, when a symbol is incorrectly detected it is possible that more than one bit error is made.

The array performance for QPSK will be very similar to that for BPSK discussed in [3]. For QPSK, the desired signal at the input to the first array element during the n^{th} symbol interval is given by

$$\tilde{d}(t) = A_d \exp\{j[\omega t + \phi_n(t) + \psi_d]\} \tag{2.19}$$

where A_d is the amplitude of $\tilde{d}(t)$, and $\phi_n(t)$ is equally likely to be any member of the set $\{0,\pi/2, \pi, 3\pi/2\}$ depending on the transmitted symbol. ψ_d, the phase of the received signal, is assumed to be a uniformly distributed random variable on $(0,2\pi)$ that is statistically independent of $\phi_n(t)$. The autocorrelation function (ACF) of $\tilde{d}(t)$ can be determined from (2.19) and (2.8) yielding,

$$R_{\tilde{d}}(\tau) = A_d^2 \left(1 - \frac{|\tau|}{T}\right) e^{-j\omega_d \tau} \tag{2.20}$$

where T is the symbol duration. It is interesting to note that this is the same ACF that we derived for the BPSK signalling case in [3].

The interference signal at the first array element is given by,

$$\tilde{i}(t) = A_i \exp\{j[\omega_i t + \psi_i]\} \tag{2.21}$$

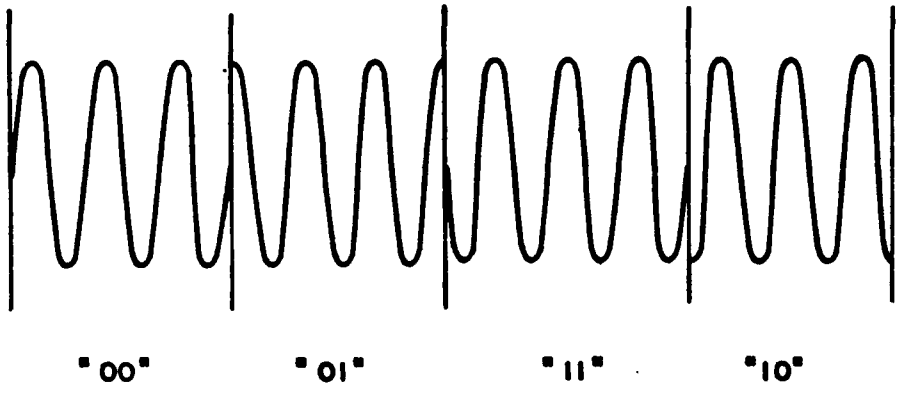

Figure 2. Typical QPSK waveform with bit-pair assignments.

where A_i is the interference amplitude and ψ_i, the interference phase, is uniformly distributed on $(0,2\pi)$ and statistically independent of ψ_d. The ACF for the interference is determined using (2.11) and (2.21) yielding,

$$\tilde{R_i}(\tau) = A_i^2 \, e^{-j\omega_i \tau} \tag{2.22}$$

Again we find that this is the same ACF as we had for the BPSK case.

From the expressions given above for the desired signal and interference ACFs, the corresonding covariance matrices can be calculated from (2.7) and (2.10). The reference correlation vector S can be calculated from (2.20) and (2.14) and the array weights can then be calculated using (2.6) and (2.1). Finally, the desired signal, interference, and noise powers at the array output can be calculated using (2.15) through (2.17). It is interesting to note that, since the desired signal and interference ACFs are the same for QPSK as they were for BPSK, the adaptive array power calculations for QPSK will be identical to those presented in [3] for BPSK.

III. QPSK DETECTOR PERFORMANCE WITH CW AND AWGN INTERFERENCE

In this section we derive the performance of an ideal QPSK detector when the QPSK desired signal is corrupted by CW interference and AWGN. The ideal QPSK detector is shown in Figure 3 [2]. This detector is ideal if the only undesired signal is AWGN. This detector is essentially two BPSK detectors in which the reference signals at the two multipliers are in phase quadrature. At the end of the n^{th} symbol

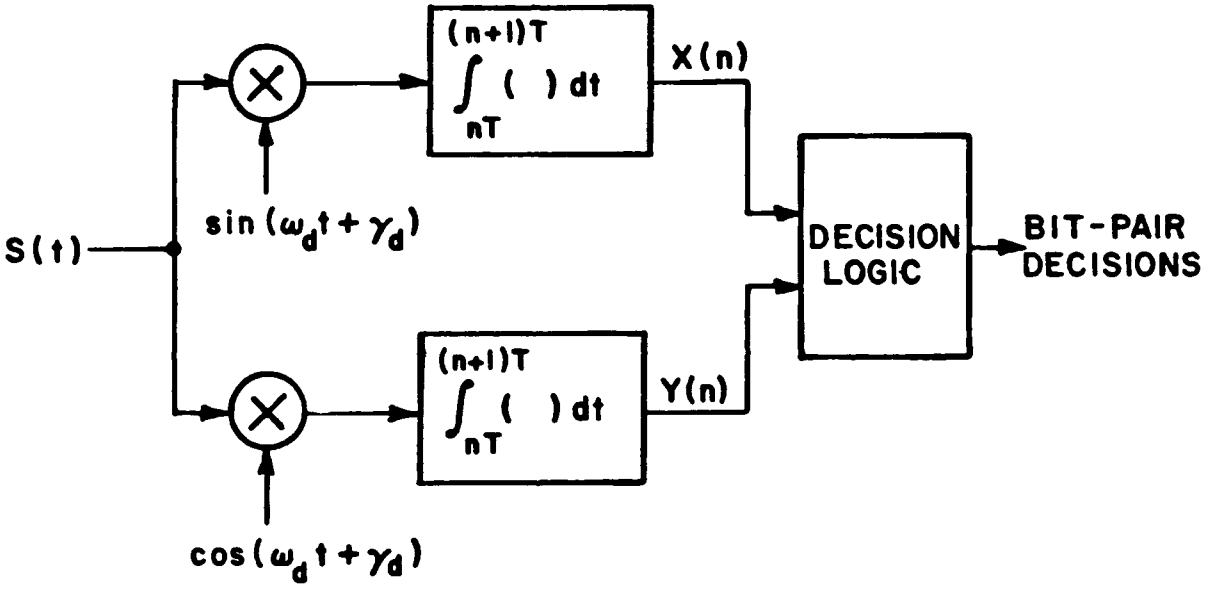

Figure 3. Ideal QPSK detector.

interval the integrator outputs, X(n) and Y(n), are examined and a symbol decision is made based upon the values at these outputs. The decision regions for the different symbols are shown in Figure 4.

In order to determine the probability of a symbol error we must first calculate the joint statistics of the integrator outputs, X(n) and Y(n). We note that the process by which X(n) is derived is identical to the process by which X(n) was derived for the ideal BPSK detector of Figure 3.3 of reference [3]. Therefore, from Equations (2.19) and (3.37) of this reference, the expression for X(n) is immediately found to be

$$X(n) = \sqrt{\frac{P_d}{2}}\, T \cos[\phi_n(t)] + \sqrt{\frac{P_i}{2}}\, \text{sinc}\left(\frac{\Delta\omega T}{2}\right) \cos\left(\gamma_{rel} + \frac{\Delta\omega T}{2}\right) + X_n(n) \tag{3.1}$$

where $\phi_n(t)$ is equally likely to be any member of the set $\{0,\pi/2,\pi,3\pi/2\}$ during any symbol interval. The noise term $X_n(n)$ is normally distributed with zero mean and variance $\eta T/4$.

We next examine Y(n) which is given by,

$$Y(n) = Y_d(n) + Y_i(n) + Y_n(n), \tag{3.2}$$

where,

$$Y_d(n) = \int_{nT}^{(n+1)T} \sqrt{2P_d}\, \sin(\omega_d t + \gamma_d)\cos[\omega_d t + \phi_n(t) + \gamma_d]dt, \tag{3.3}$$

$$Y_i(n) = \int_{nT}^{(n+1)T} \sqrt{2P_i}\, \sin[\omega_d t + \gamma_d]\cos[\omega_i t + \gamma_i]dt, \tag{3.4}$$

and,

$$Y_n(n) = \int_{nT}^{(n+1)T} s_n(t)\sin[\omega_d t + \gamma_d]dt. \tag{3.5}$$

As in Chapter 3 of reference [3] we will evaluate each of these three integrals and then combine the results to determine Y(n). The limits of integration are also simplified by setting n = 0.

It is easily shown using standard trigonometric identities that $Y_d(n)$ reduces to,

$$Y_d(n) = -\sqrt{\frac{P_d}{2}}\, T \sin[\phi_n(t)]. \tag{3.6}$$

The second integral to be evaluated, $Y_i(n)$, is given by,

$$Y_i(n) = \sqrt{\frac{P_i}{2}} \int_0^T \sin[(\omega_d + \omega_i)t + \gamma_d + \gamma_i] + \sin[(\omega_d - \omega_i)t + \gamma_d - \gamma_i]dt, \tag{3.7}$$

We drop the double frequency term yielding,

$$Y_i(n) = \sqrt{\frac{P_i}{2}} \int_0^T \sin(\Delta\omega t + \gamma_{rel})dt, \tag{3.8}$$

where $\Delta\omega = \omega_d - \omega_i$, $\gamma_{rel} = \gamma_d - \gamma_i$ and T is the symbol duration. Evaluating this integral we have

$$Y_i(n) = \sqrt{\frac{P_i}{2}} \left(\frac{1}{\Delta\omega}\right)[\cos(\gamma_{rel}) - \cos(\Delta\omega T + \gamma_{rel})], \tag{3.9}$$

which can be simplified using standard trigonometric identities yielding

$$Y_i(n) = \sqrt{\frac{P_i}{2}}\, T\, \mathrm{sinc}\left(\frac{\Delta\omega T}{2}\right) \sin\left[\gamma_{rel} + \frac{\Delta\omega T}{2}\right]. \qquad (3.10)$$

We denote the noise signal at the integrator output at the end of the n^{th} symbol interval by $Y_n(n)$. It is straightforward to show that $Y_n(n)$ is a zero mean gaussian random variable with variance $\frac{nT}{4}$ (where $\frac{n}{2}$ is the PSD of the noise at the detector input). A nearly identical analysis is given in [3] where the statistics of $X_n(n)$ are derived.

Furthermore, if we assume that the PSD of the noise at the detector input is symmetric about ω_d, then $X_n(n)$ and $Y_n(n)$ will be independent of each other at the end of each symbol interval. This property is easily shown using the standard decomposition of narrowband noise into quadrature components [5]. The values of $X_n(n)$, $Y_n(n)$, $X_n(m)$, and $Y_n(m)$ will be uncorrelated (and thus independent) for $m \neq n$.

The desired, interfering, and noise signals at the integrator output can now be combined using (3.2), (3.6) and (3.10) yielding,

$$Y(n) = -\sqrt{\frac{P_d}{2}}\, T \sin[\phi_n(t)] + \sqrt{\frac{P_i}{2}}\, T\, \mathrm{sinc}\left(\frac{\Delta\omega T}{2}\right) \sin\left(\gamma_{rel} + \frac{\Delta\omega T}{2}\right) + Y_n(n), \qquad (3.12)$$

where $Y_n(n)$ is a zero mean normal random variable with variance $\frac{nT}{4}$.

The probability of a symbol error P(e) can be calculated using the expressions for X(n) and Y(n) given by (3.1) and (3.12), and the decision regions shown in Figure 4. If we assume equally likely symbols, then P(e) is given by

$$P(e) = \frac{1}{4}\left[P[e|\phi_n(t) = 0] + P[e|\phi_n(t) = \frac{\pi}{2}]\right.$$

$$\left. + P[e|\phi_n(t) = \pi] + P[e|\phi_n(t) = \frac{3\pi}{2}]\right] \quad (3.13)$$

The symmetry of the decision regions and the nature of X(n) and Y(n) insure that the probability of a symbol error be will independent of which symbol is transmitted (for equally likely symbols). Therefore the probablity of error is,

$$P(e) = P[e|\phi_n(t) = 0] \quad (3.14)$$

If $\phi_n(t) = 0$ then X(n) and Y(n) become,

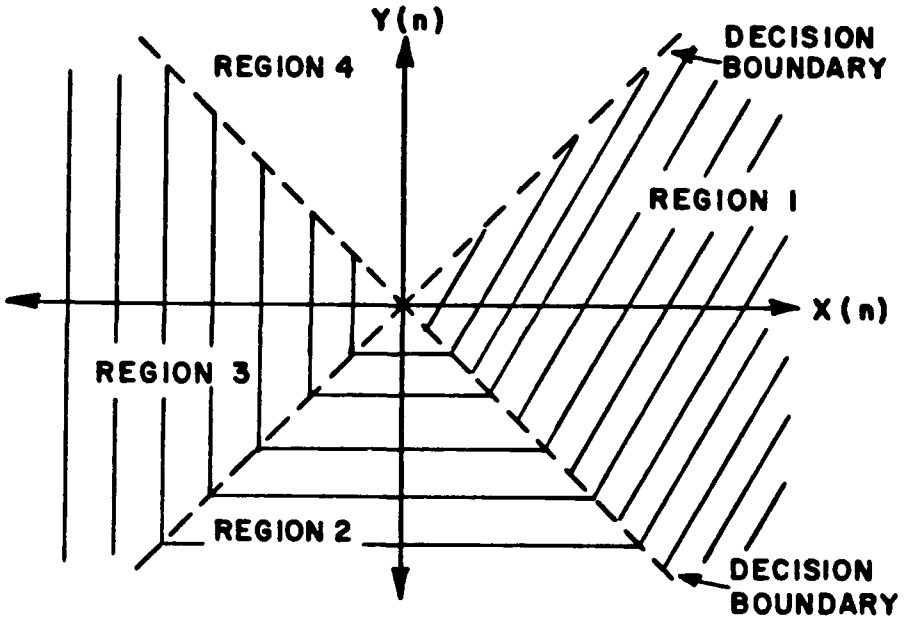

Figure 4. QPSK decision space.

$$X(n) = \sqrt{\frac{P_d}{2}}\, T + \sqrt{\frac{P_i}{2}}\, T\ \mathrm{sinc}\ (\frac{\Delta\omega T}{2})\ \cos(\gamma_{rel} + \frac{\Delta\omega T}{2}) + X_n(n), \quad (3.15)$$

and,

$$Y(n) = \sqrt{\frac{P_i}{2}}\, T\mathrm{sinc}\ (\frac{\Delta\omega T}{2})\ \sin(\gamma_{rel} + \frac{\Delta\omega T}{2}) + Y_n(n). \quad (3.16)$$

The problem of calculating P(e) for QPSK given X(n) and Y(n) is very similar to a problem addressed by Rosenbaum [6] and we will use similar notation and procedures for ease of comparison. We first normalize X(n) and Y(n) by dividing each by $\sqrt{\frac{P_d}{2}}\, T$ yielding

$$X' = 1 + b\cos(\gamma_{rel} + \frac{\Delta\omega T}{2}) + n_x, \quad (3.17)$$

and,

$$Y' = b\sin(\gamma_{rel} + \frac{\Delta\omega T}{2}) + n_y, \quad (3.18)$$

where,

$$b = \sqrt{\frac{P_i}{P_d}}\ \mathrm{sinc}(\frac{\Delta\omega T}{2}), \quad (3.19)$$

and n_x and n_y are independent and identically distributed normal random variables with zero mean and variance,

$$\sigma_{xy}^2 = \frac{(\eta T/4)}{(P_d T^2/2)}$$

$$= \frac{1}{(2E_d/\eta)}\ . \quad (3.20)$$

The normalized variables X' and Y' are shown on the decision space diagram in Figure 5.

Since X' and Y' are independent jointly gaussian random variables, their joint probability density function (PDF) conditioned on γ_{rel} is,

$$f_{xy}(X',Y'|\gamma_{rel}) = \frac{1}{2\pi\sigma_{xy}^2} \exp\left[\frac{-1}{2\sigma_{xy}^2}[(X' - b\sin\gamma)^2 + (Y' - 1 - b\cos\gamma)^2]\right] \quad (3.21)$$

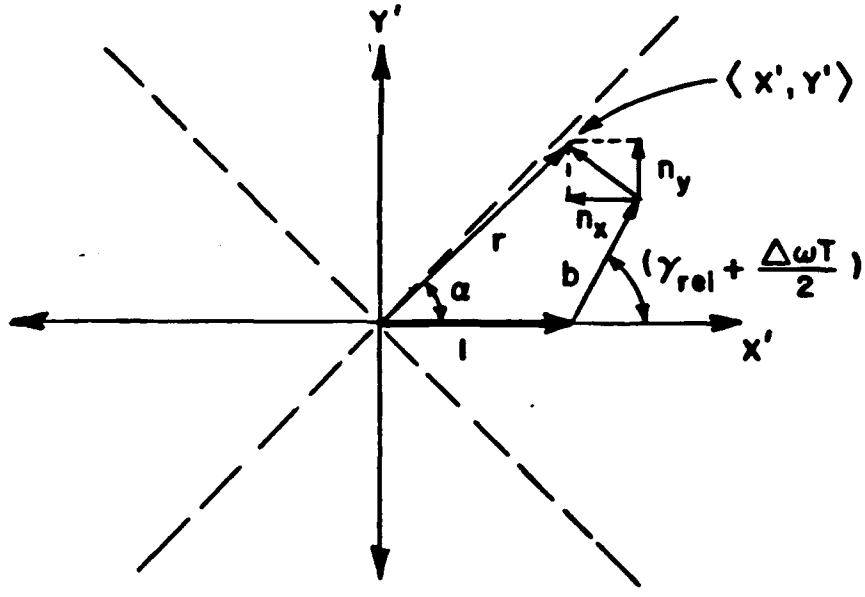

Figure 5. Normalized decision space showing composite received signal.

where,

$$\gamma = \gamma_{rel} + (\frac{\Delta\omega T}{2}). \tag{3.22}$$

The dependence of this PDF of γ can be eliminated by integrating the product of $f_{xy}(X',Y'|\gamma_{rel})$ and $\frac{1}{2\pi}$ (the PDF of the uniformly distributed variable γ) yielding,

$$f_{xy}(X',Y') = (\frac{1}{2\pi\sigma_{xy}})^2 \exp[\frac{-1}{2\sigma_{xy}^2}[(X'^2 + (Y'-1)^2 + b^2]]$$

$$\cdot \int_0^{2\pi} \exp\,[\frac{b}{2\sigma_{xy}^2}[\sqrt{X'^2 + (Y'-1)^2}\cos(\gamma+\Gamma)]]d\gamma, \tag{3.23}$$

where $\Gamma = \tan\,(\frac{Y'-1}{X'})$ is not a function of γ.

This expression can be simplified after recognizing the integral yielding,

$$f_{xy}(X',Y') = (\frac{1}{2\pi\sigma_{xy}})^2 \exp[\frac{-1}{2\sigma_{xy}^2}[(X'^2 + (Y-1)^2 + b^2]]$$

$$\cdot I_0\{\frac{b}{2\sigma_{xy}^2}\sqrt{X'^2 + (Y'-1)^2}\} \tag{3.24}$$

where I_0 is the modified Bessel function of the first kind of order zero.

We can now change from rectangular to polar coordinates using the transformation,

$$X = r\sin(\alpha), \tag{3.25}$$

and,

$$Y = r\cos(\alpha). \tag{3.26}$$

The geometrical interpretation of r and α are shown in Figure 5. To implement the transformation we perform the indicated change of variables, and multiply the resulting function by the Jacobian of the transformation, r. We can then eliminate the dependency on r by integrating the density over all possible values of r. The resulting expression will be the probability density function of the angle α. This PDF is given by,

$$f_\alpha(\alpha) = \frac{1}{2\pi\sigma_{xy}^2} \int_0^\infty \exp\left[\frac{-1}{2\sigma_{xy}^2}\left[r^2 + b^2 + 1 - 2r\cos\alpha\right]\right]$$

$$\cdot I_0\left\{\frac{b}{2\sigma_{xy}^2}\sqrt{r^2 + 1 - 2r\cos\alpha}\right\} r\,dr. \tag{3.27}$$

The probability of error, P(e) will be given by the probability that α does not lie between $\frac{-\pi}{4}$ and $\frac{\pi}{4}$ when $\phi_n(t)=0$. Thus P(e) is given by,

$$P(e) = \int_{-\pi}^{-\pi/4} f_\alpha(\alpha)d\alpha + \int_{\pi/4}^{\pi} f_\alpha(\alpha)da \tag{3.28}$$

From the symmetry of the integrand it is seen that (3.28) can be rewritten,

$$P(e) = 2\int_{\pi/4}^{\pi} f_\alpha(\alpha)d\alpha \tag{3.29}$$

Equation (3.29) was evaluated numerically for several SNR and INR values. Results of these calculations are shown (for $\Delta\omega T=0$) in Figures

6 and 7*. The integrals were evaluated using Simpson's rule where the Bessel function was evaluated using either a polynomial or an asymptotic approximation depending on the magnitude of the argument. From Figures 6 and 7 we see that these curves are similar to the curves shown in reference [3] for BPSK. However, P(e), the probability of a symbol error is higher for QPSK. We should remember that each symbol in the QPSK symbol stream represents two bits of information. Thus, for QPSK, it is possible for one symbol error to produce two bit errors.

It should also be noted that the detector shown in Figure 3 is the ideal detector for M-ary PSK with AWGN. The only change required is the division of the decision space into M regions. The probability of error for M-ary PSK is given by (3.29) with the lower limit of integration changed to $\frac{\pi}{M}$.

IV. PERFORMANCE OF THE COMBINED LMS ARRAY/QPSK DETECTOR

In this section we will combine the results of the previous two sections in order to determine the overall performance of a QPSK detector that is preceded by an LMS adaptive array. Again in this section we will find that the required derivations closely parallel those of Section 3 in [3]. Also, as mentioned previously the adaptive array calculations are identical for BPSK and QPSK signaling. The only difference in the performance of the two systems will be caused by the differences in the BPSK and QPSK detectors.

---

*Figures 6 and 7 show the same data as a function of two different independent variables. Similarly, two sets of pltos will be given for each case we consider in this report.

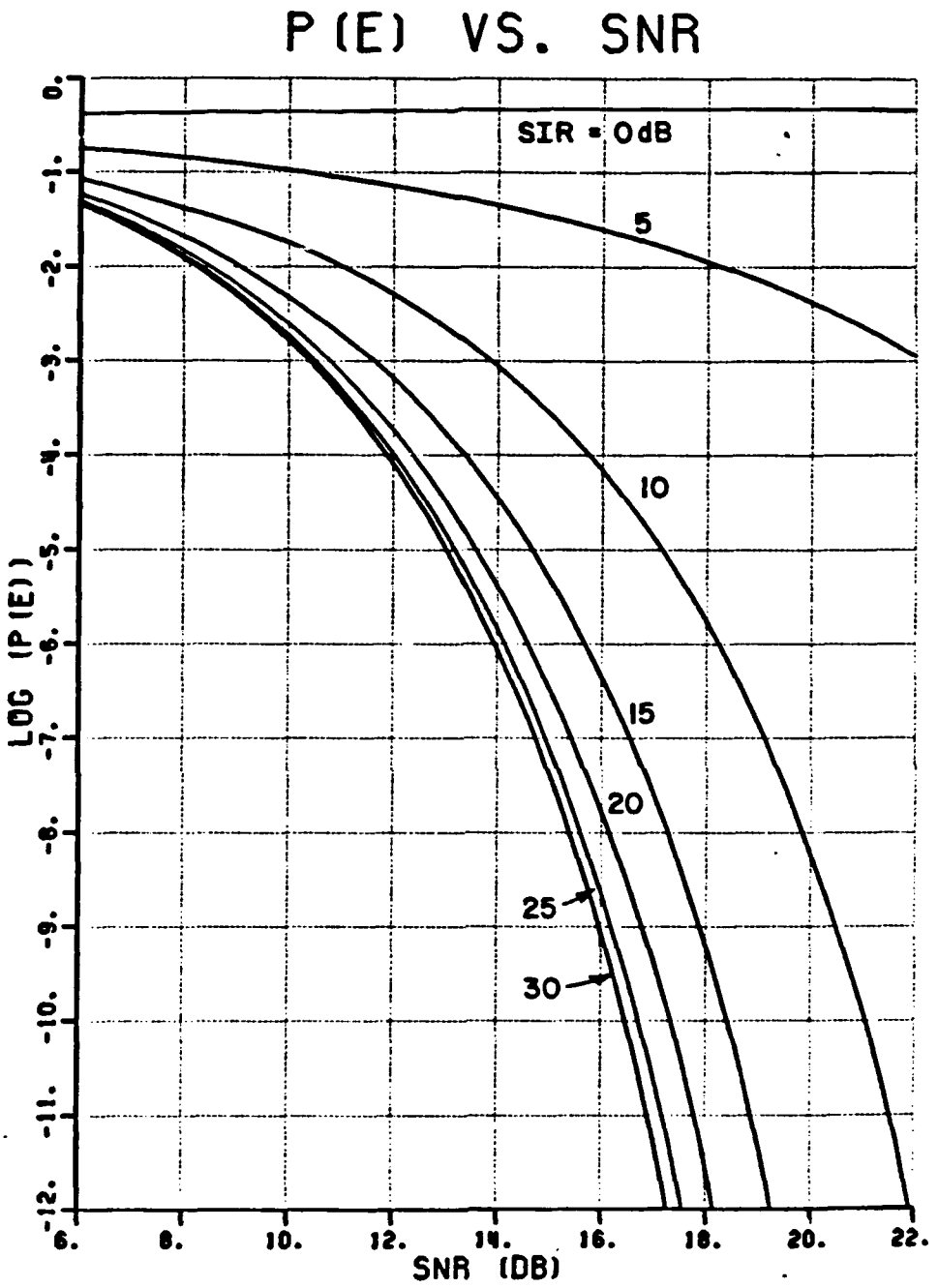

Figure 6. QPSK detector performance for several SIR values.

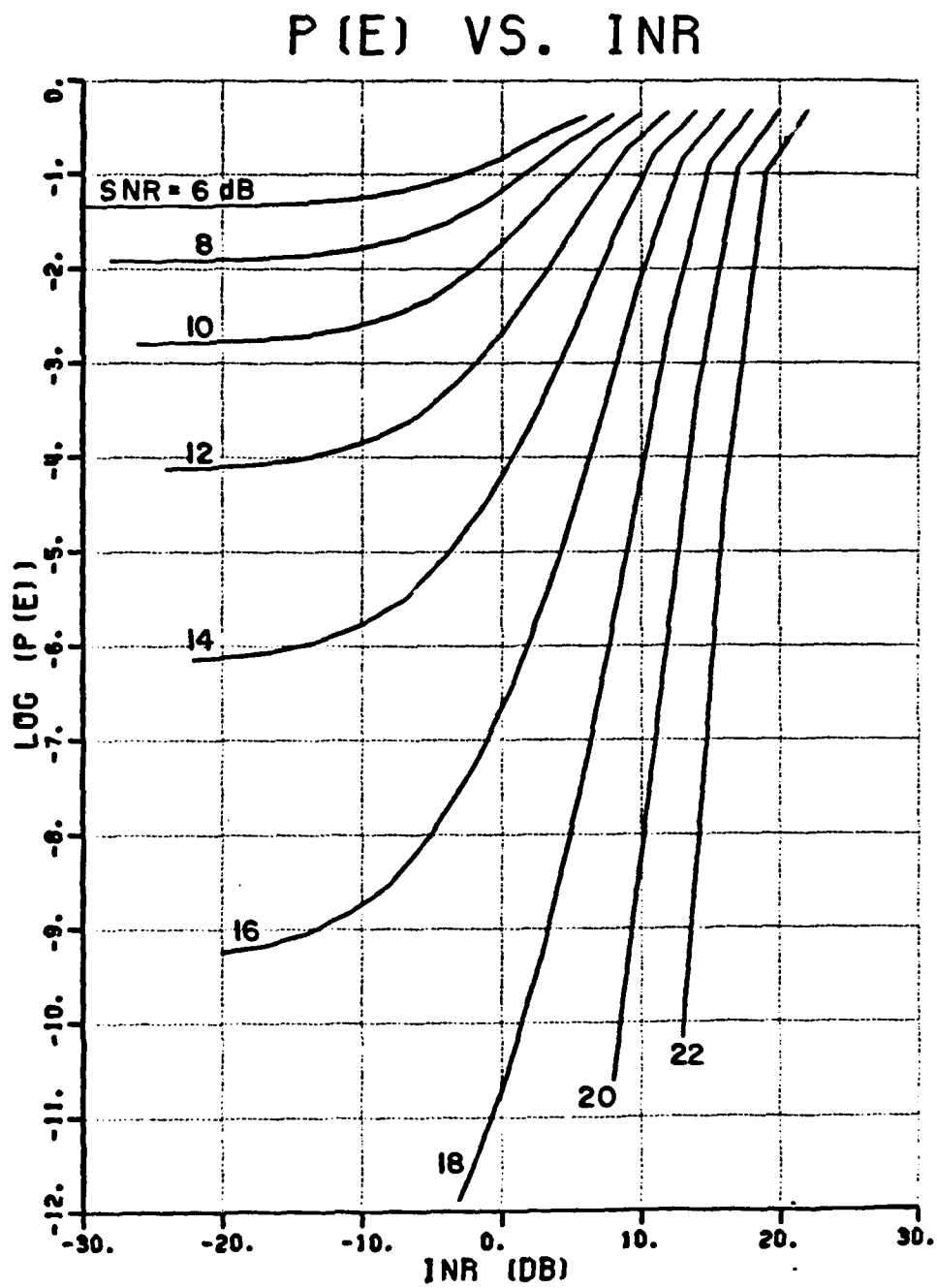

Figure 7. QPSK detector performance for several SNR values.

Six variables are required to specify the system performance. These variables are:

$(E_d)_{in}/N_o$ = the input SNR at each element input where $(E_d)_{in}$ is the desired signal energy-per-bit-interval at each element input and $N_o/2$ is the 2-sided noise PSD.

$(E_i)_{in}/N_o$ = the input INR at each element input where $(E_i)_{in}$ is the interference energy-per-bit-interval at each element input and $N_o/2$ is the 2-sided noise PSD.

θ_d = the desired signal arrival angle.

θ_i = the interference arrival angle.

k = the array bandwidth factor. k is the ratio of the input noise bandwidth to (2/T) Hz., the width of the main peak in the desired signal spectrum.

$\Delta\omega T$ = the change in phase of the interference signal with respect to the desired signal during each bit interval.

From these 6 variables the amplitudes of the desired and interfering signals at the array inputs and the noise power at each element input can be calculated. The noise power at the element inputs will be equal to the product of the noise spectral density and the array bandwidth. Therefore, for a fixed noise spectral density, the noise power at each element will be directly proportional to k.

In this report we examine the system performance for k values of 5 and 10. For these k values, the BPFs at the element inputs do not significantly distort the desired signal. Furthermore, over the range of frequencies for which the detector is sensitive, the noise PSD will be constant. Therefore the signal and detector models described in the previous section are appropriate.

The performance of the LMS array and QPSK detector was calculated for several scenarios. Results are shown in Figures 8 through 20. Figures 8 and 9 show the performance of the system with θ_d=0° and θ_i=10°. The array bandwidth factor k was set equal to 5 and the interference phase offset per symbol $\Delta\omega T$ was set equal to zero (i.e. the interference frequency was set equal to the desired signal center frequency). Figures 10 through 13 show similar results for θ_i values of 20 and 80 degrees.

The results shown in these figures illustrate the interference protection afforded by the adaptive array. The curves shown in Figures 8 through 13 are very similar in shape to the curves shown in [3] for the BPSK case and the discussions of the BPSK results contained in this reference are directly applicable here. The P(e) values for QPSK are larger for QPSK than for BPSK in all cases. This is not surprising since QPSK signaling generally produces higher P(e) values than BPSK. However, in return for these higher error rates, QPSK offers twice the data rate of BPSK for a fixed transmission bandwidth.

The humps in the P(e) vs. INR curves are easily explained. At low INR values the thermal noise is stronger than the interference at the

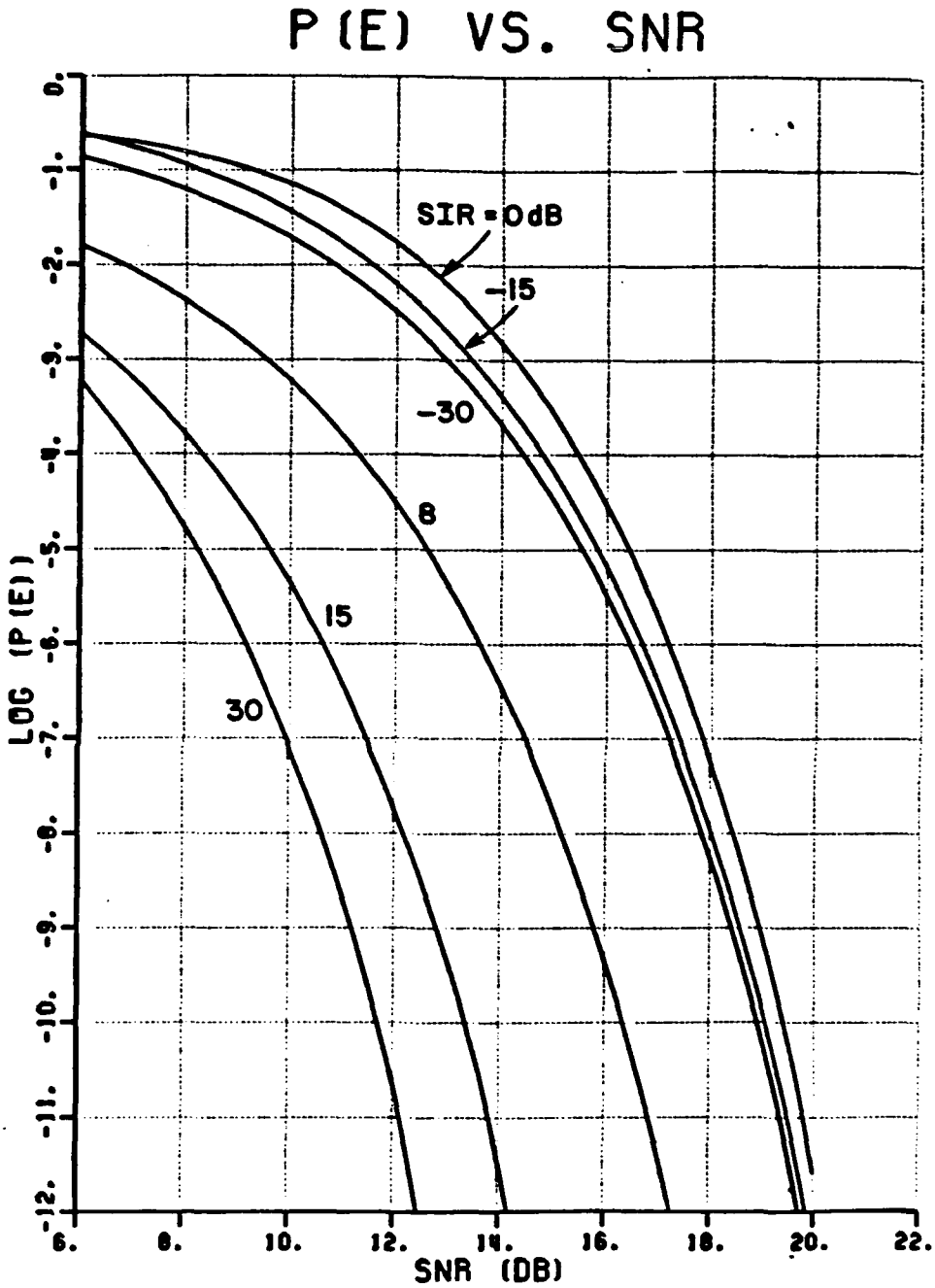

Figure 8. QPSK P(e) vs. SNR for 3-element array (θ_j=10°, k=5, $\Delta\omega T$=0).

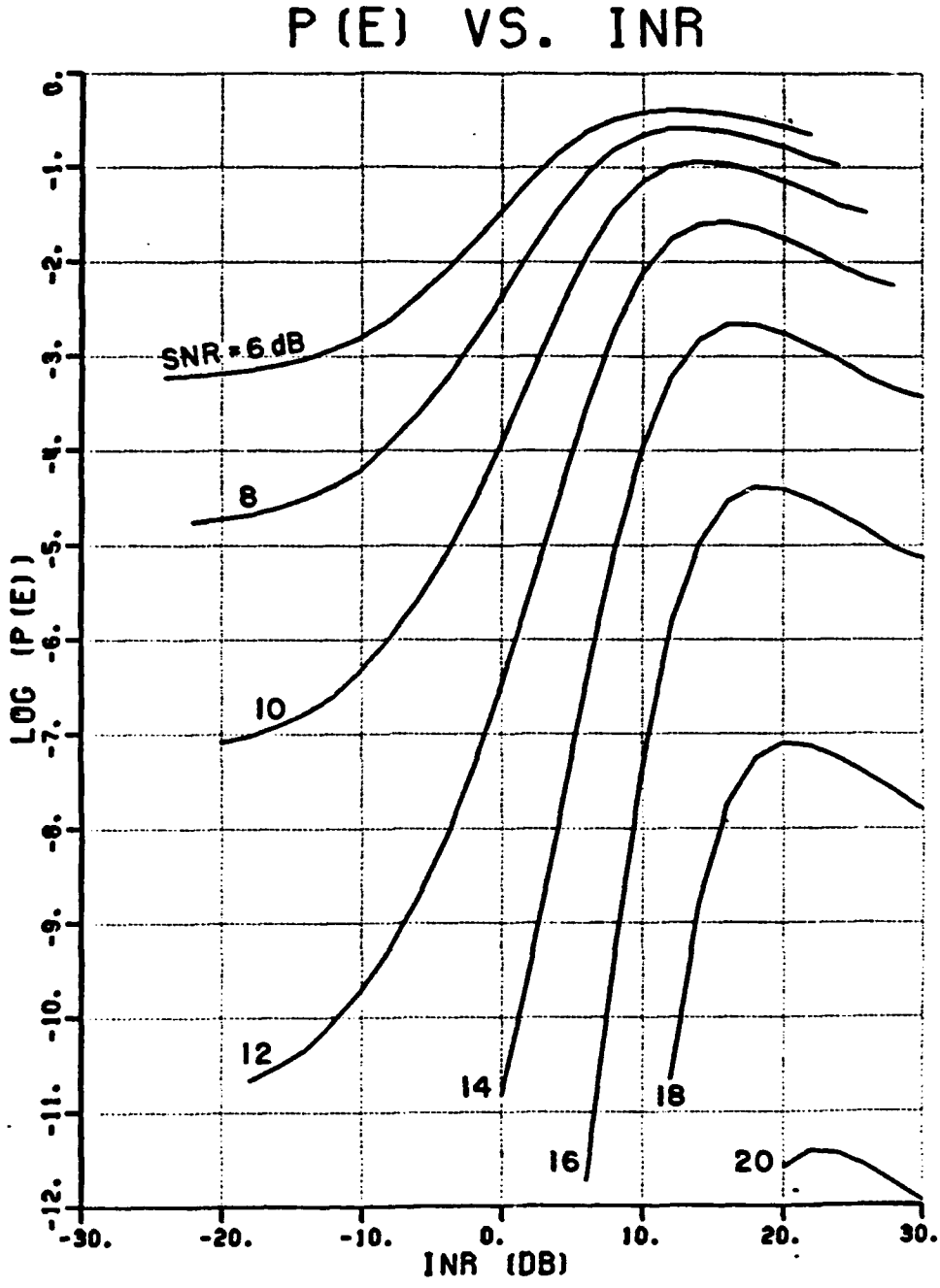

Figure 9. QPSK P(e) vs. INR for 3-element array (θ_j=10°, k=5, $\Delta\omega T$=0).

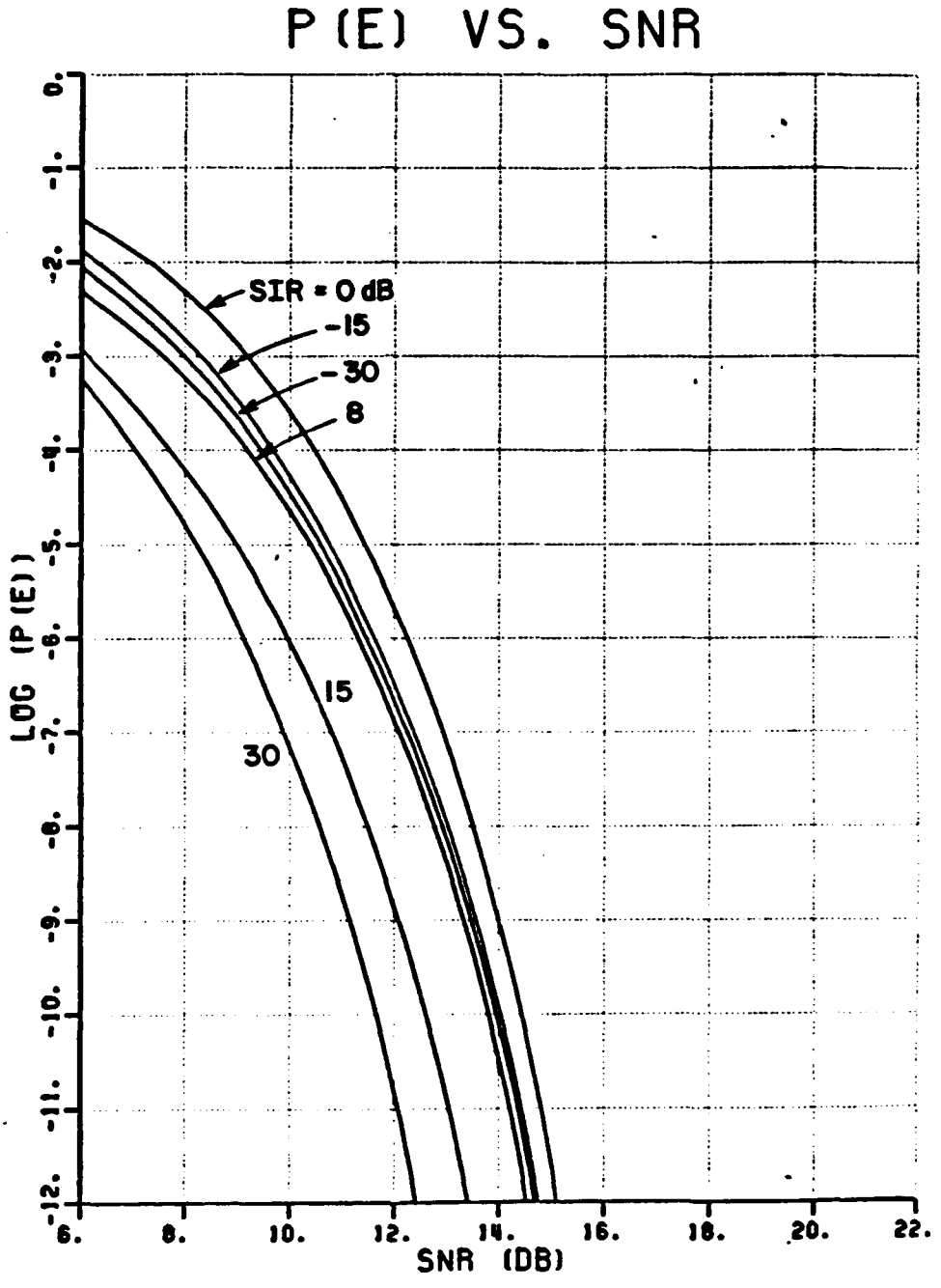

Figure 10. QPSK P(e) vs. SNR for 3-element array (θ_j=20°, k=5, $\Delta\omega T$=0).

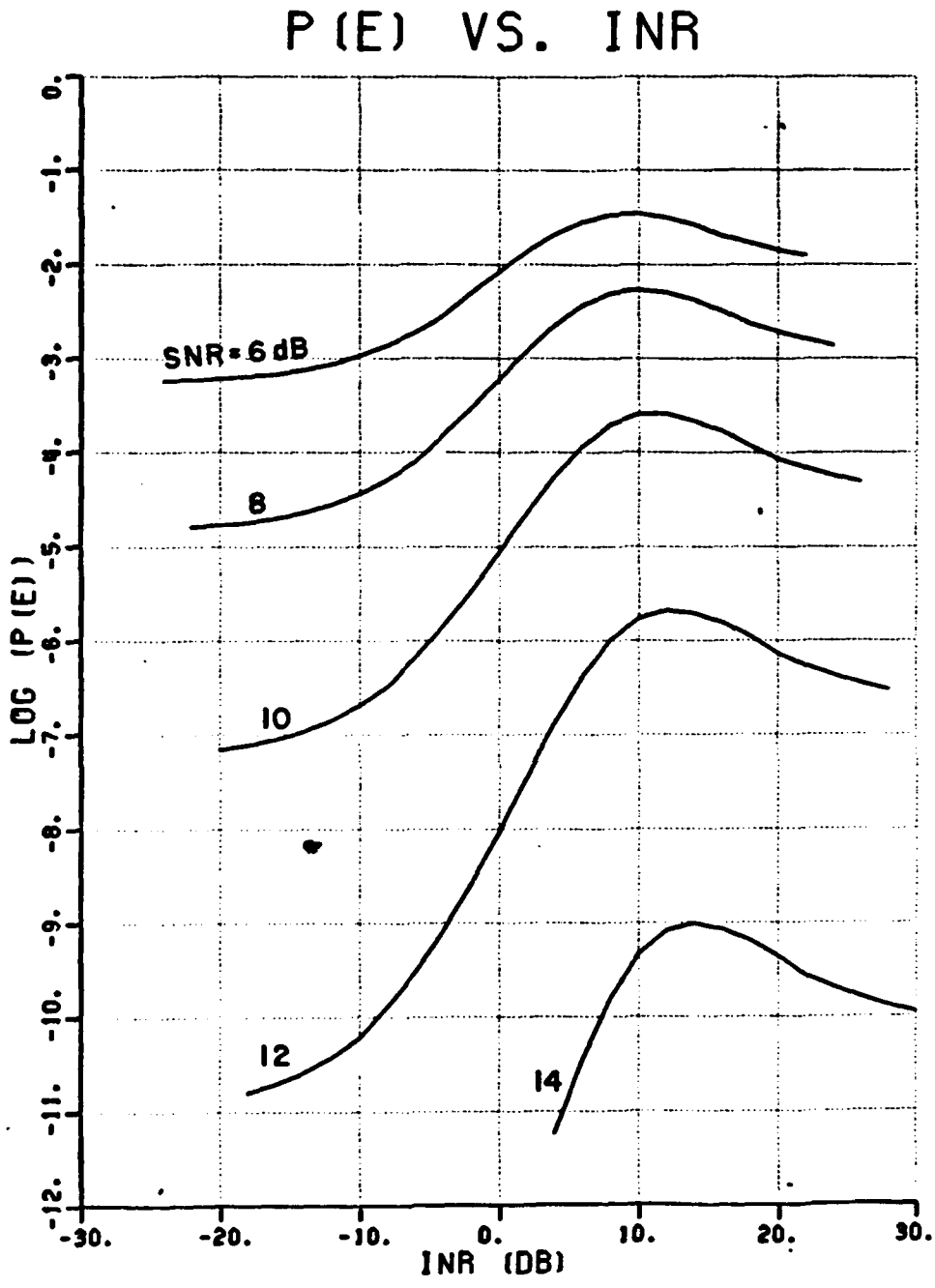

Figure 11. QPSK P(e) vs. INR for 3-element array (θ_j=20°, k=5, $\Delta\omega T$=0).

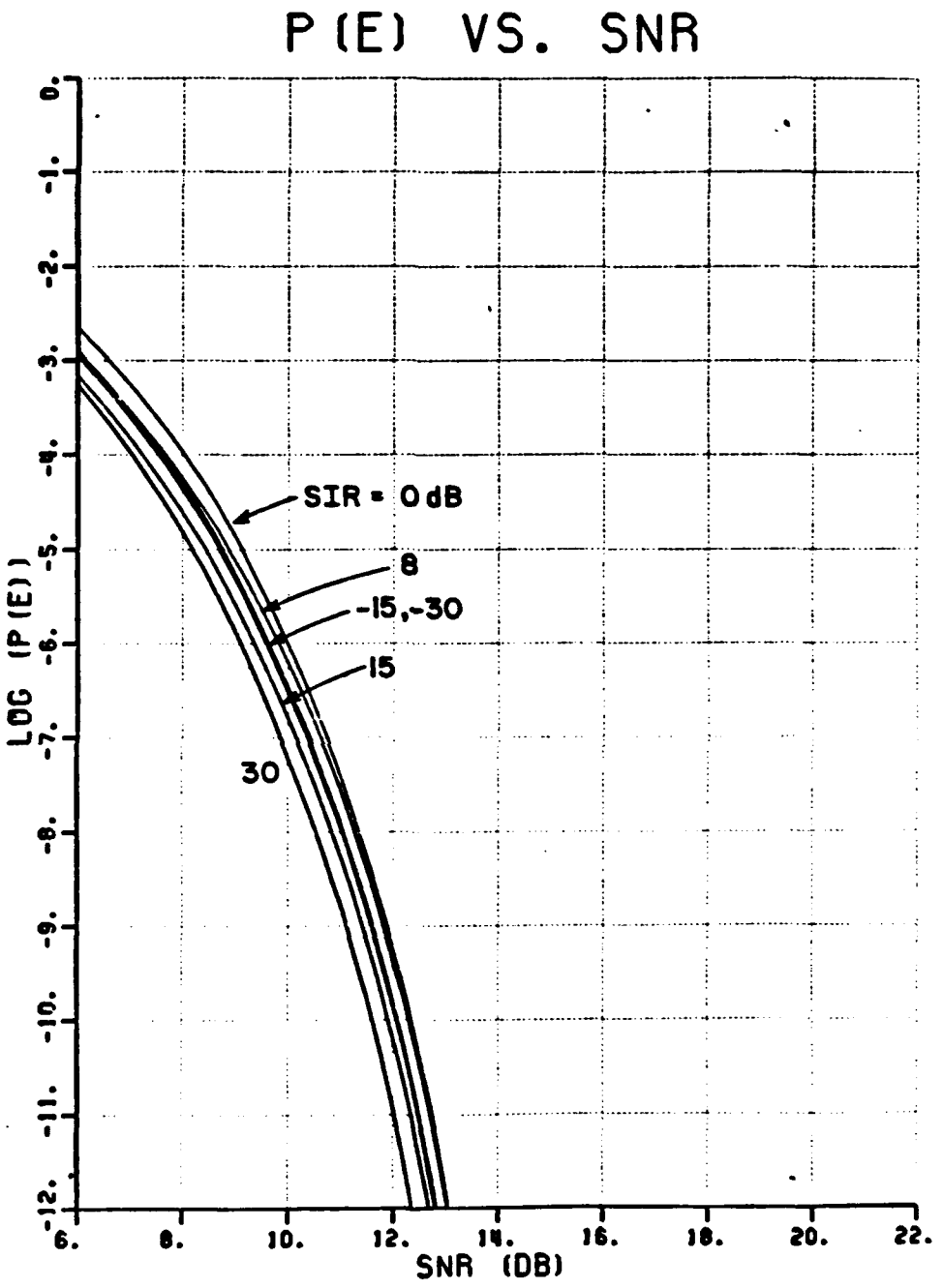

Figure 12. QPSK P(e) vs. SNR for 3-element array (θ_j=80°, k=5, $\Delta\omega T$=0).

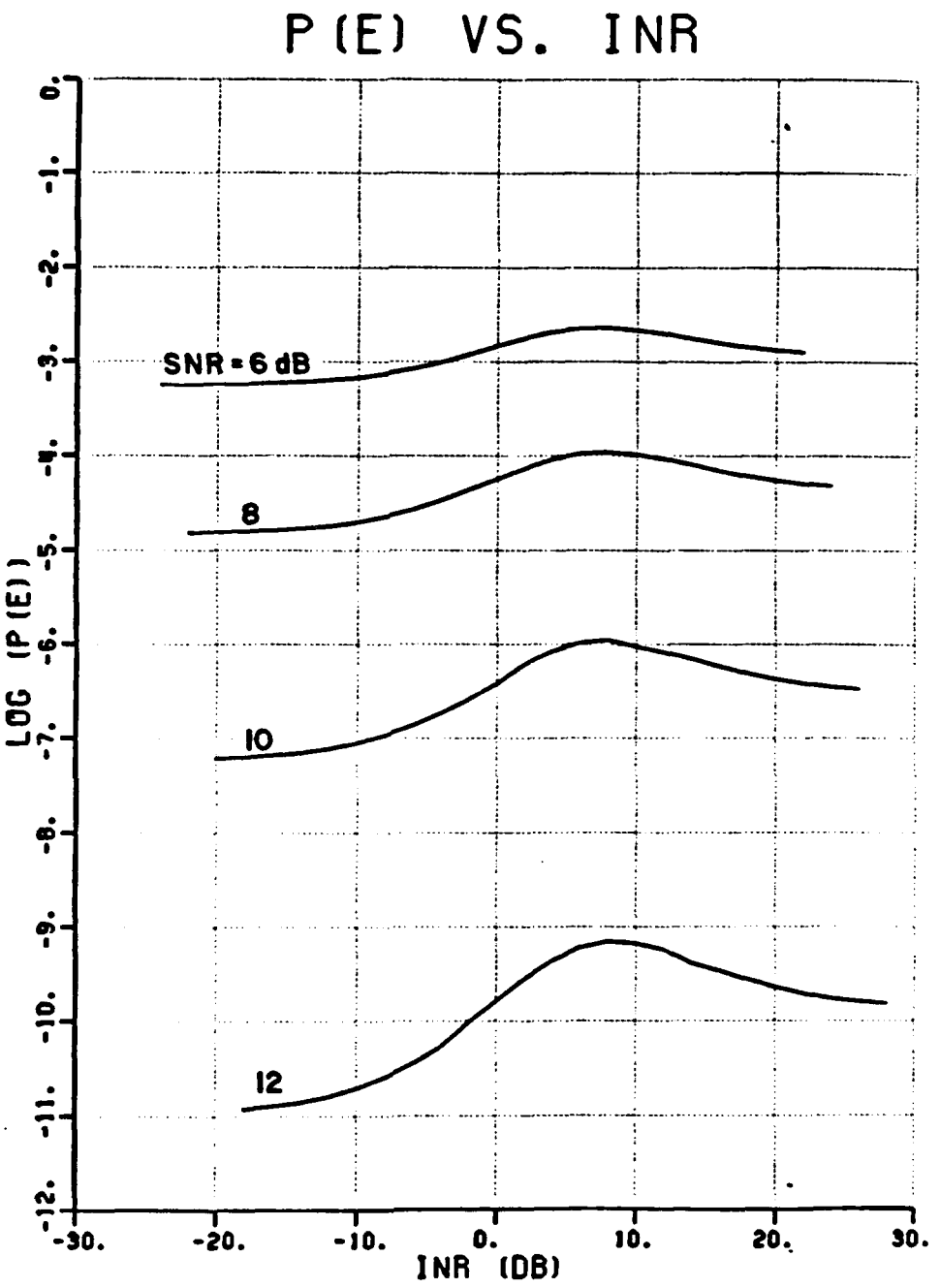

Figure 13. QPSK P(e) vs. INR for 3-element array (θ_j=80°, k=5, $\Delta\omega T$=0).

array inputs. As the INR increases, the interference power at the array output and P(e) both increase. As the INR increases above approximately 10 dB the array begins to null the jammer. As the INR is increased further this null becomes deeper and a point is reached where any additional increase in input interference power produces a corresponding decrease in the interference power at the array output. At high INR values, a very deep null is formed in the interfering signal direction.

One of the arrays degrees of freedom is used to create the deep null for high INR levels. With its remaining degrees of freedom, the array can no longer keep the desired signal at a pattern maximum. Therefore the array performance at very high input INR values is not as good as it is at very low INR value even though the interference power at the array output is negligible in both cases. Adding elements to the array would increase the available degrees of freedom and therefore we would expect improved performance with a larger array.

Examination of Figures 8 through 13 indicates that the performance improves as the spatial separation between the desired and interfering signals is increased. This result is not surprising since the resolution capabilities of a three element array are somewhat limited.

Figures 14 through 19 show performance curves when the array input bandwidth is doubled (to k=10). All other parameters remain unchanged from the cases shown in Figures 8 through 13. From these figures we see that the humps in the P(e) vs. INR curves become significantly larger as the bandwidth is increased. This finding is to be expected since the

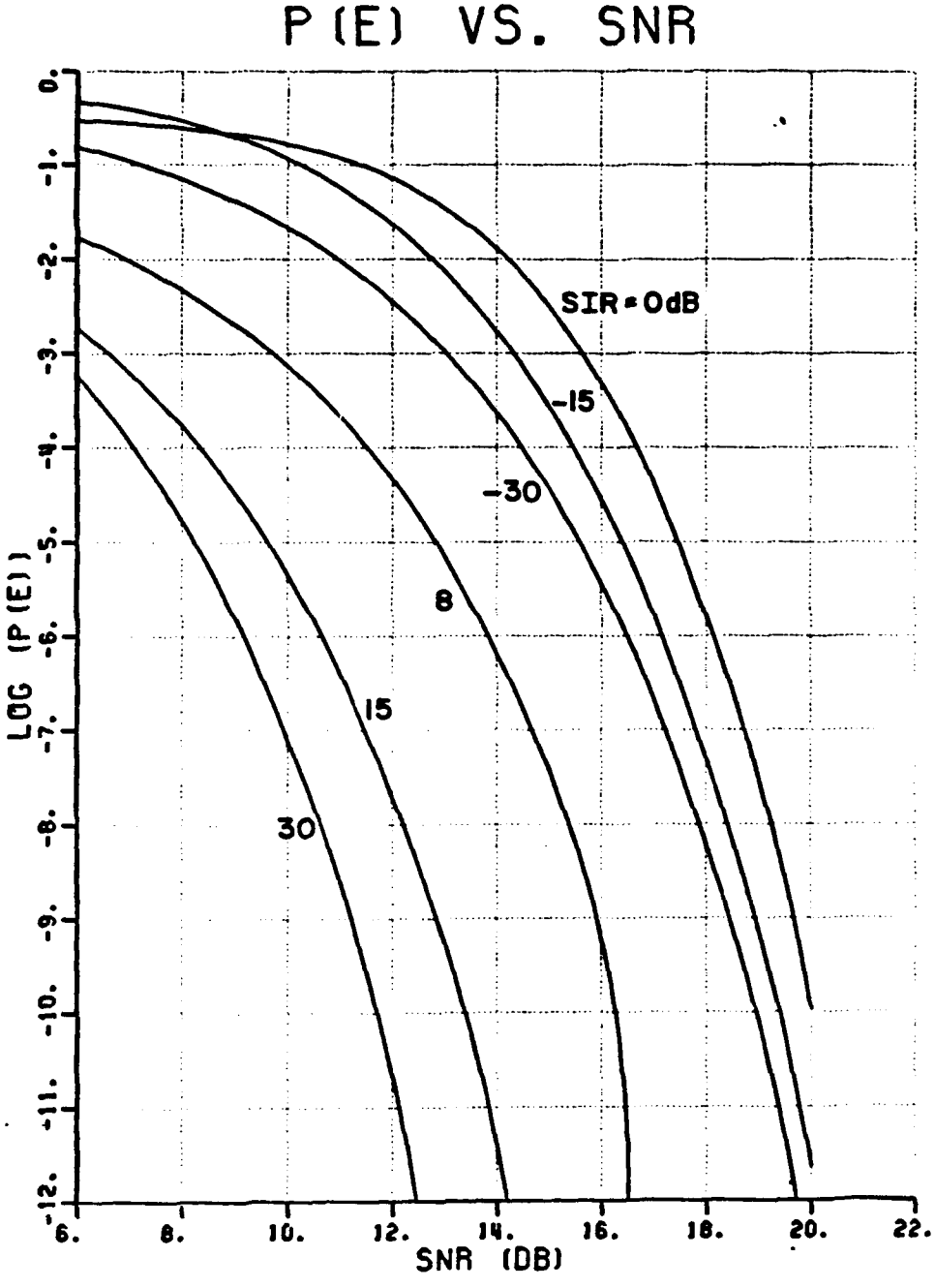

Figure 14. QPSK P(e) vs. SNR for 3-element array (θ_j=10°, k=10, $\Delta\omega T$=0).

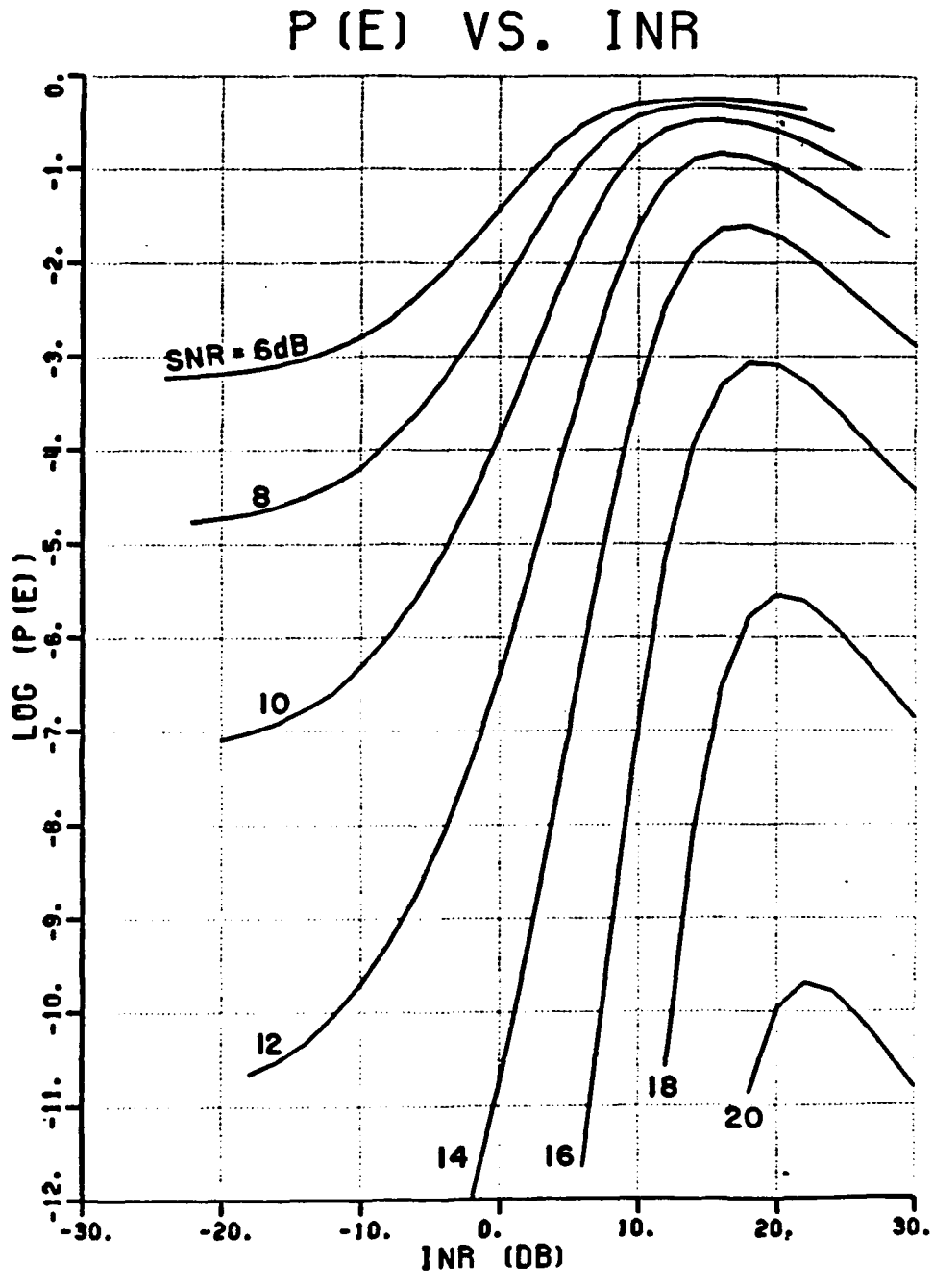

Figure 15. QPSK P(e) vs. INR for 3-element array (θ_j=10°, k=10, $\Delta\omega T$=0).

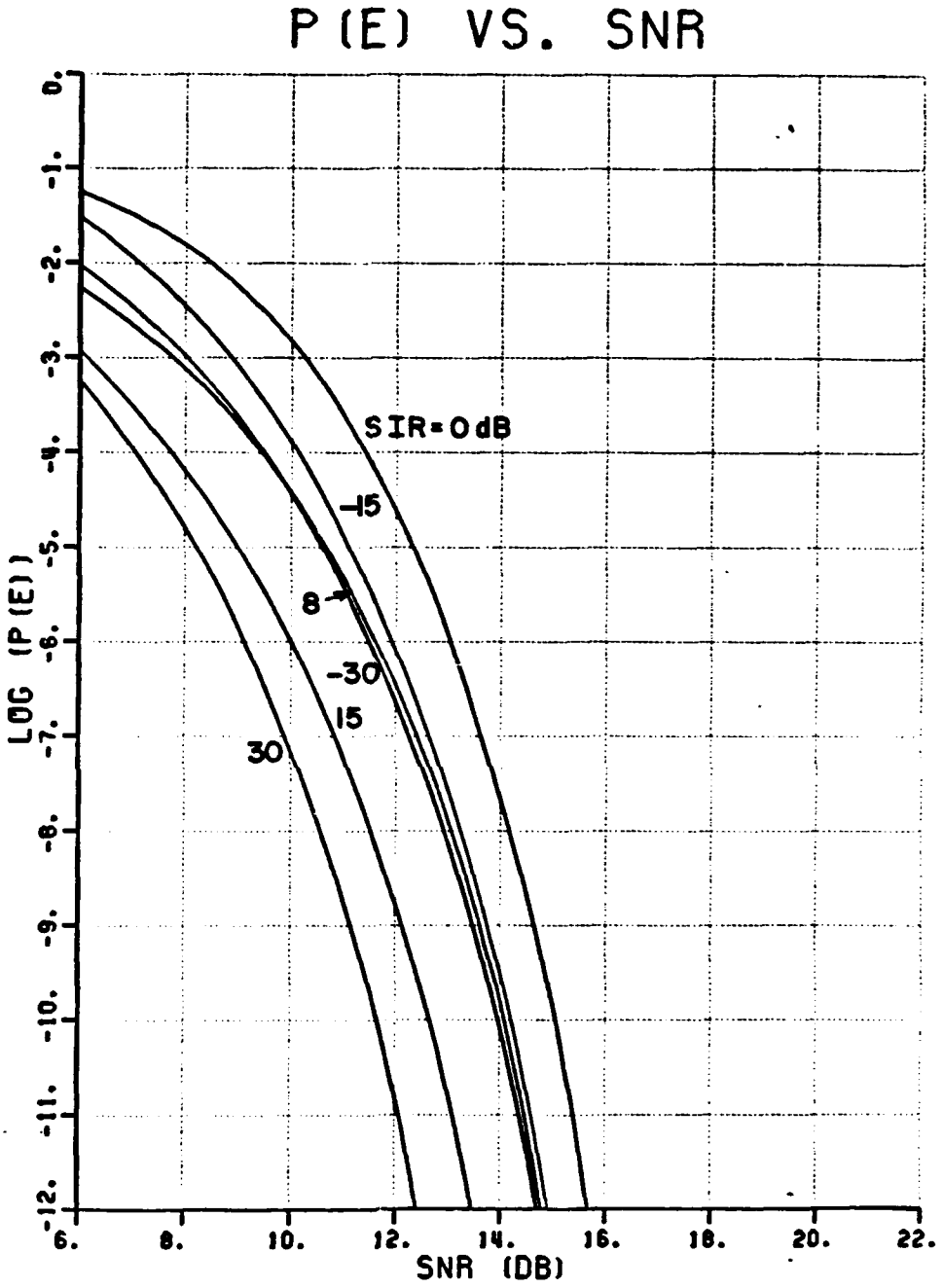

Figure 16. QPSK P(e) vs. SNR for 3-element array (θ_i=20°, k=10, $\Delta\omega T$=0).

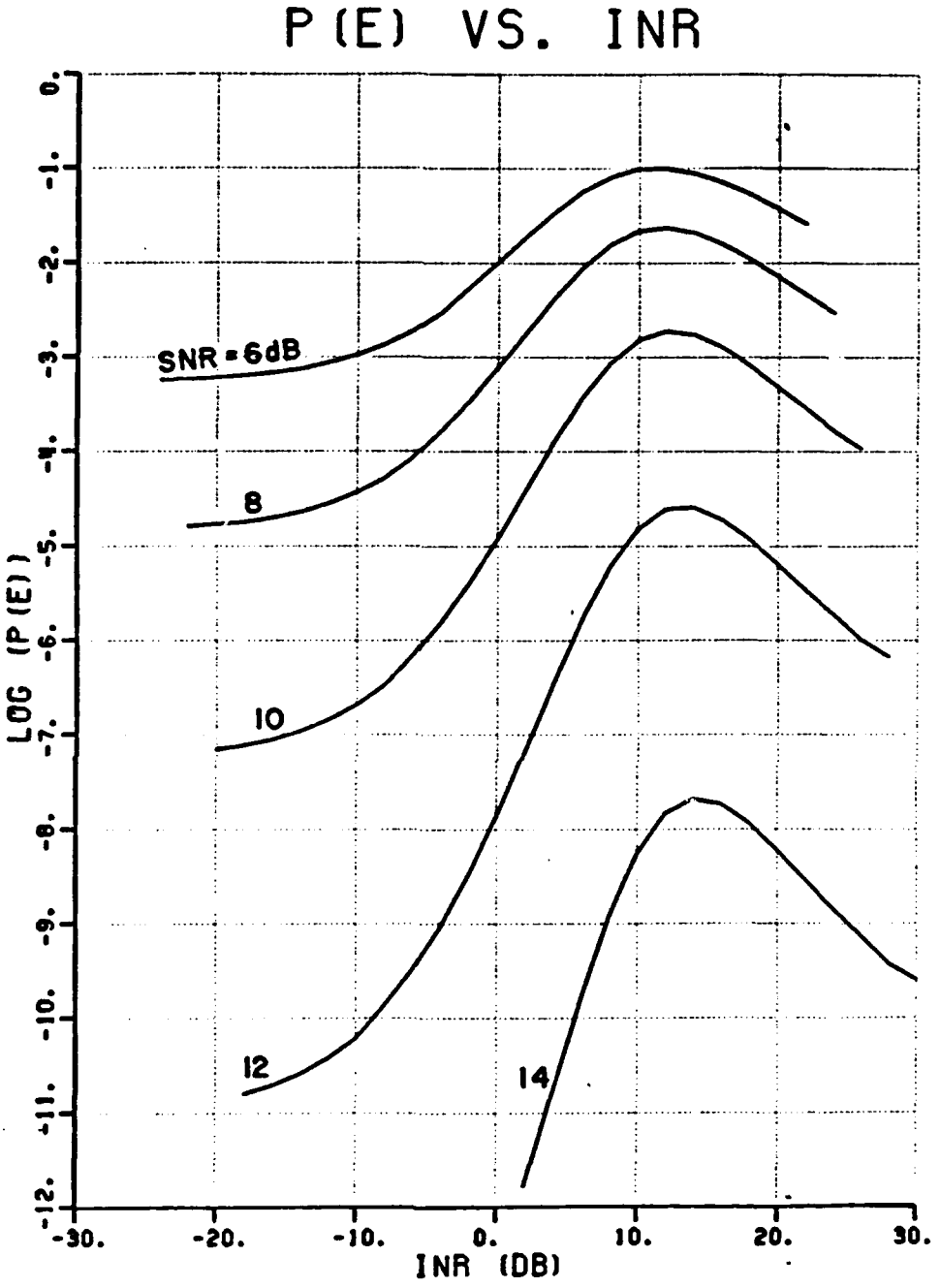

Figure 17. QPSK P(e) vs. INR for 3-element array (θ_j=20°, k=10, $\Delta\omega T$=0).

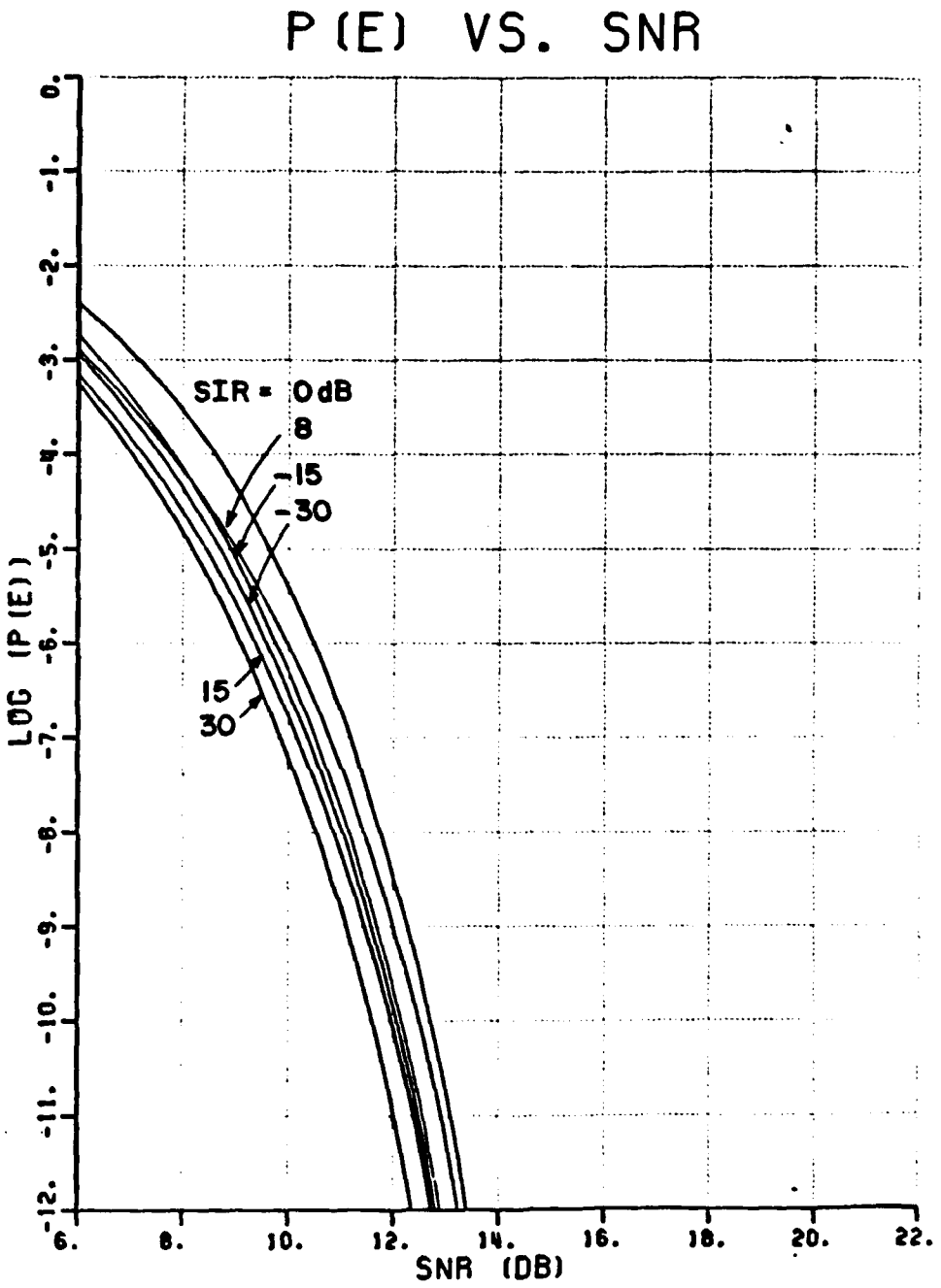

Figure 18. QPSK P(e) vs. INR for 3-element array (θ_i=80°, k=10, $\Delta\omega T$=0).

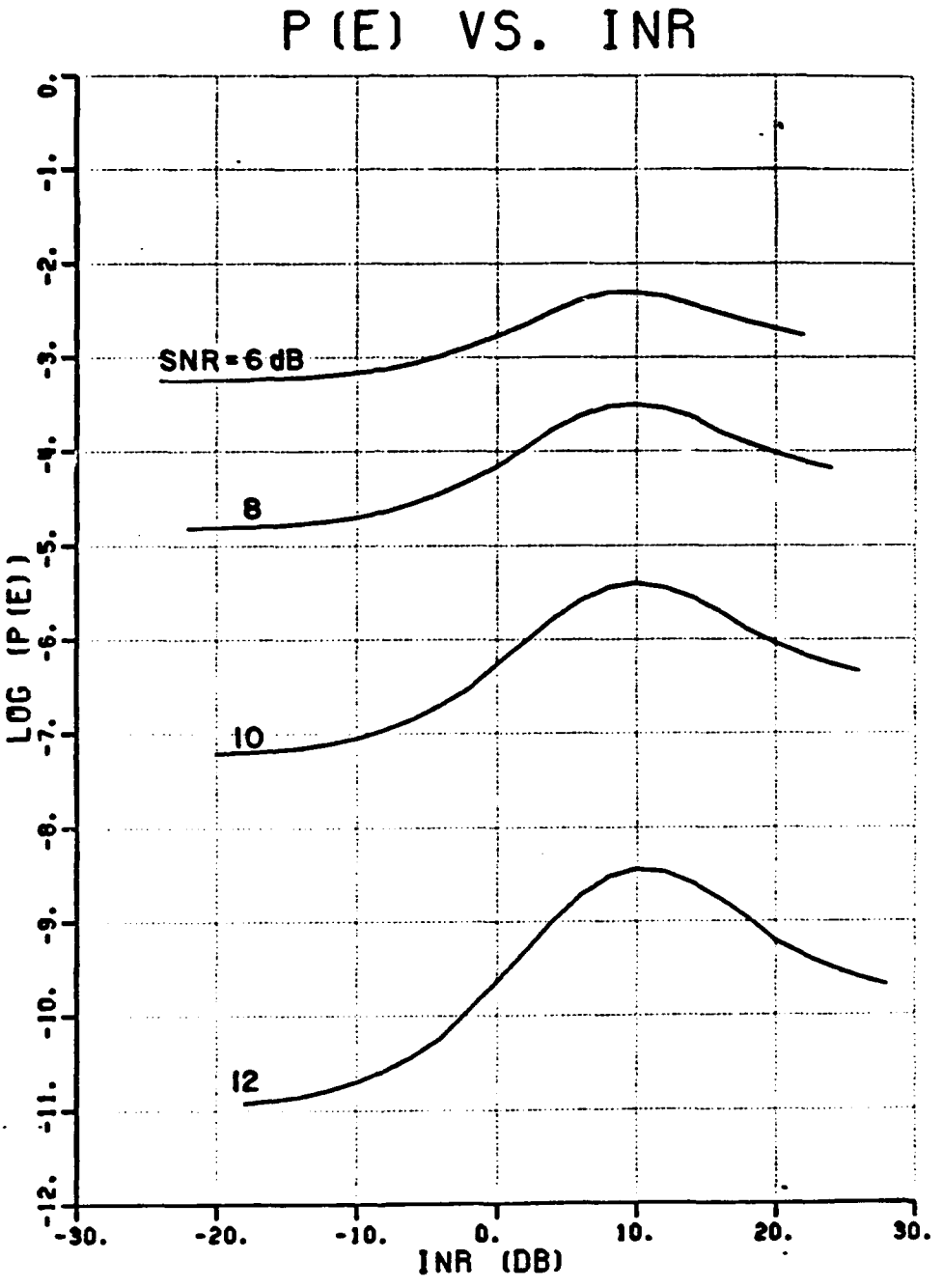

Figure 19. QPSK P(e) vs. INR for 3-element array (θ_j=80°, k=10, $\Delta\omega T$=0).

larger bandwidth allows more noise to enter the array. Therefore the INR level at which the array begins to null the interference is higher than in the previous case where k=5. For this value of INR, the interference power at the array output (and thus the P(e)) is larger than for the similar case where k=5.

Figures 20 and 21 show the performance with k=10 and the interference phase shift per symbol $\Delta\omega T$, set equal to 2π. For this case the array still responds to the interference but the detector is immune to the interference (since the interference terms in (3.15) and (3.16) are zero). The P(e) vs. INR curves for this case do not have the characteristic humps since the residual interference power at the array output does not affect the detector. The drop in SNR at the array output as the array forms a null on the interference causes the poorer performance decrease as the INR increases.

V. CONCLUSIONS

In this report we have examined the performance of a QPSK communication system that uses an adaptive array for protection from CW interference. In all respects we found the behavior of the QPSK system to be very similar to that of the BPSK system described in [3]. We found that the array provides a significant degree of protection to the system. It was found that the system performance was dependent upon several factors. First, the system performs best when there is a large spatial separation between the desired and interfering signals. It was

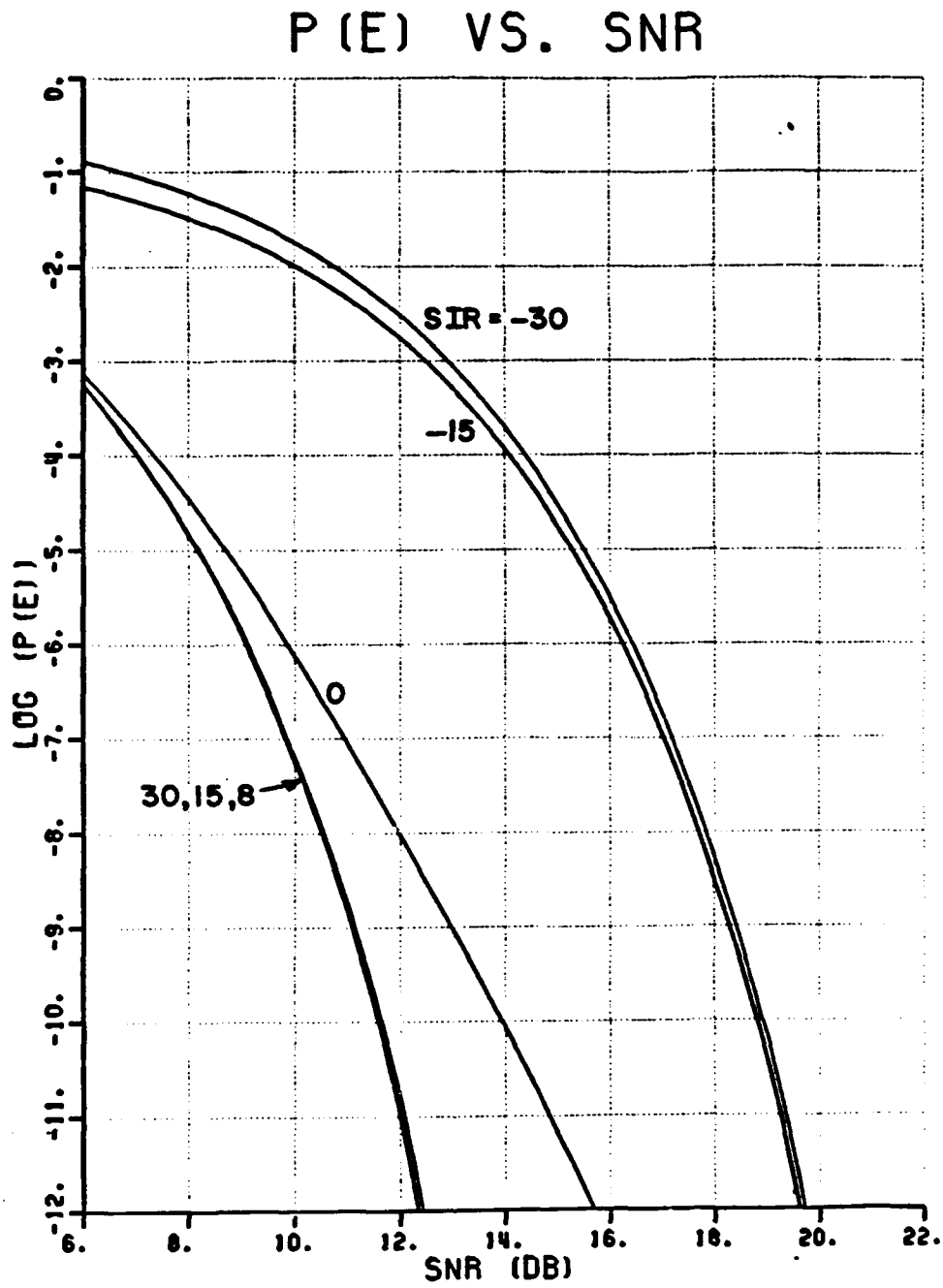

Figure 20. QPSK P(e) vs. SNR for 3-element array (θ_j=10°, k=10, $\Delta\omega T=2\pi$).

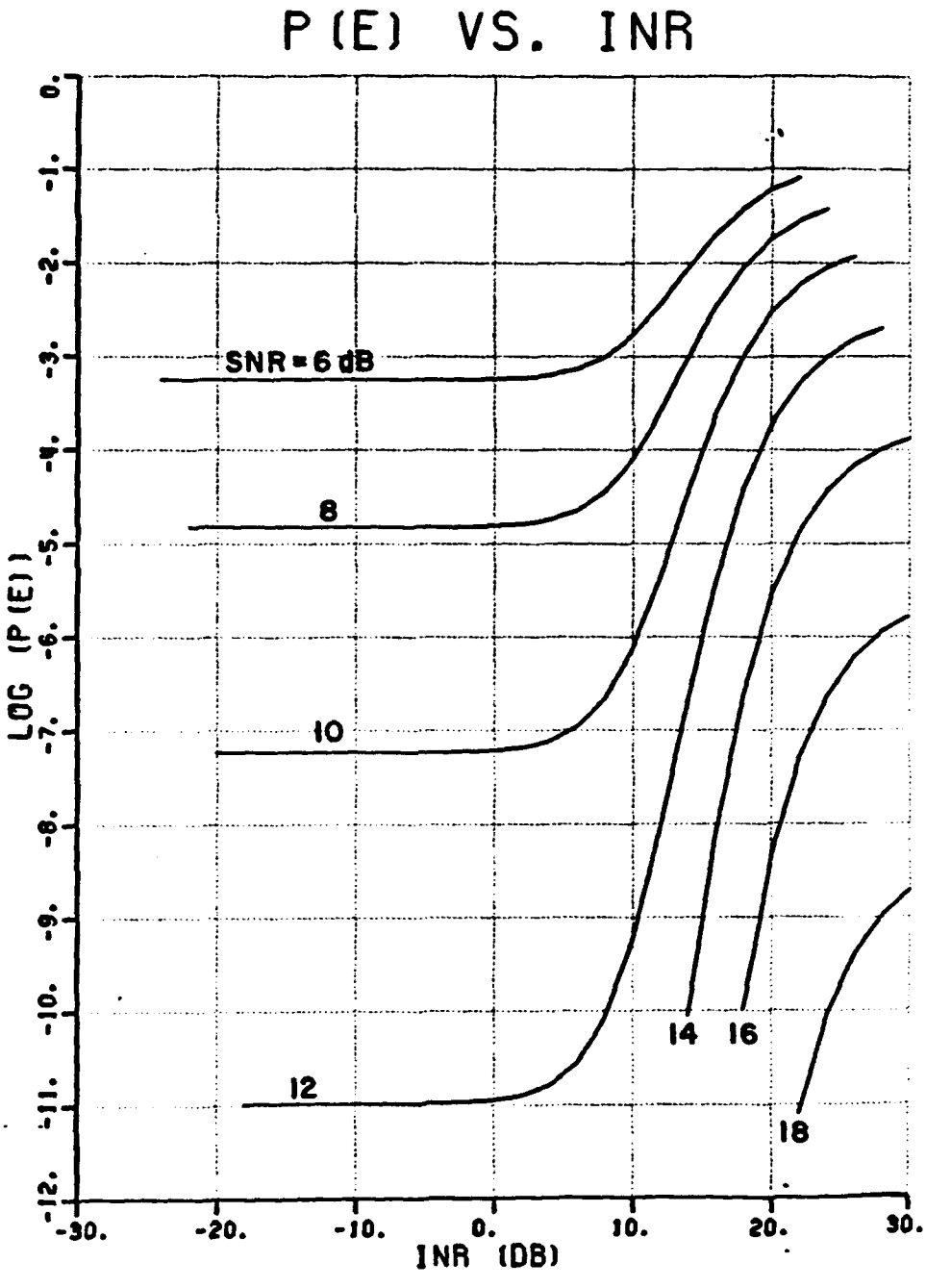

Figure 21. QPSK P(e) vs. INR for 3-element array (θ_j=10°, k=10, $\Delta\omega T=2\pi$).

also found that, for the array bandwidth considered, the system performs best with either very weak or very strong interference.

The largest error probabilities were observed for moderately powered interference. The performance for such interference was found to improve as the array bandwidth was decreased. However, the optimum array bandwidth was not determined in this report since the signal and detector models used are not appropriate for very narrow bandwidth systems. Current research efforts are being directed toward the modeling of narrowband systems. The results from these studies should indicate the system bandwidth that offers optimal protection to communication systems using adaptive arrays in the presence of both CW and broadband noise interference.

REFERENCES

[1] Widrow, B., Mantey, P.E., Griffiths, L.J., and Goode, B.B., "Adaptive Antenna Systems", Proc. IEEE, 55, 12, December 1967, p. 2143.

[2] Van Trees, H.L., Detection, Estimation, and Modulation Theory - Part I, New York, John Wiley and Sons, 1968.

[3] Ganz, M.W., "Protection of a BPSK Communication System with an LMS Adaptive Array", Report 717253-1, The Ohio State University ElectroScience Laboratory, Columbus, Ohio, October 1985.

[4] Winters, J.H., "Spread Spectrum in a Four-phase Communication System Employing Adaptive Arrays", IEEE Trans. COM-30, May 1982.

[5] Ziemer, R.E., and Tranter, W.H., Principles of Communications, Boston, Houghton Mifflin, 1976, Chapter 5.

[6] Rosenbaum, A.S., "PSK Error Performance with Gaussian Noise and Interference", Bell System Tech. Journal, Vol. 48, February 1969, pp. 413-442.